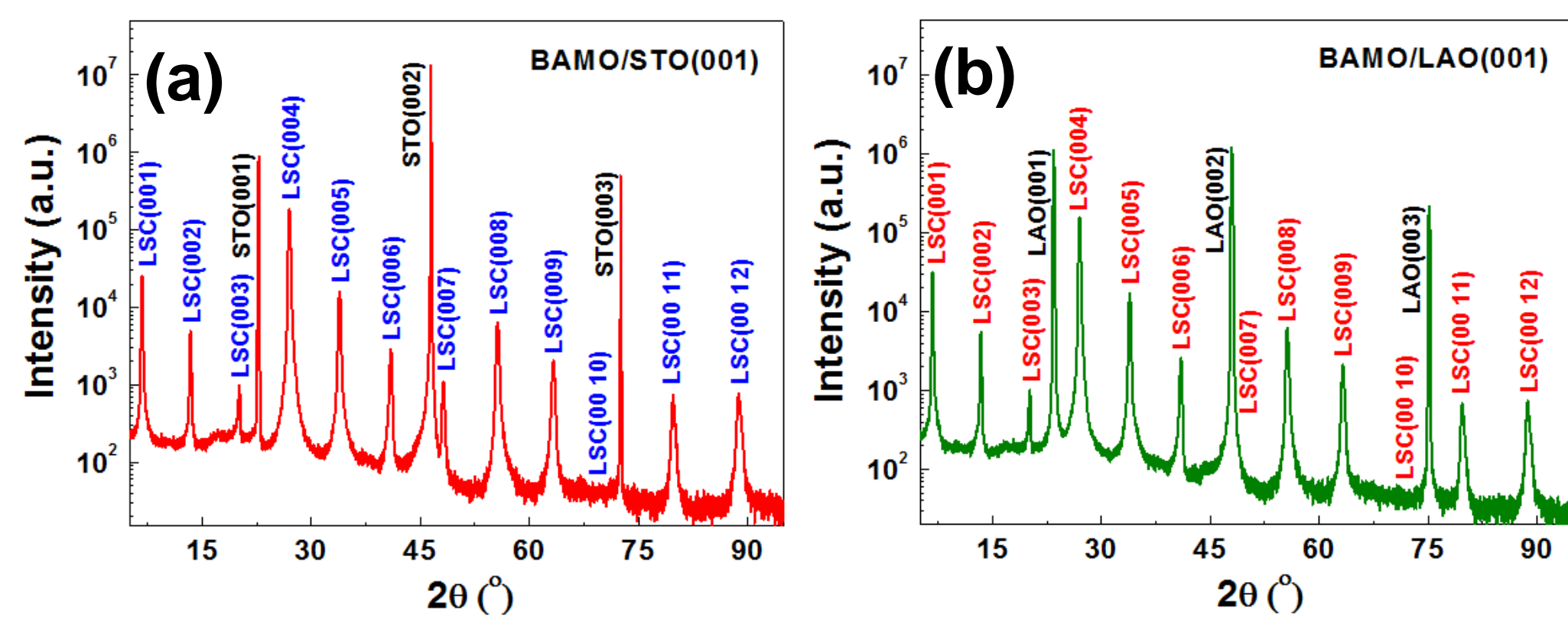
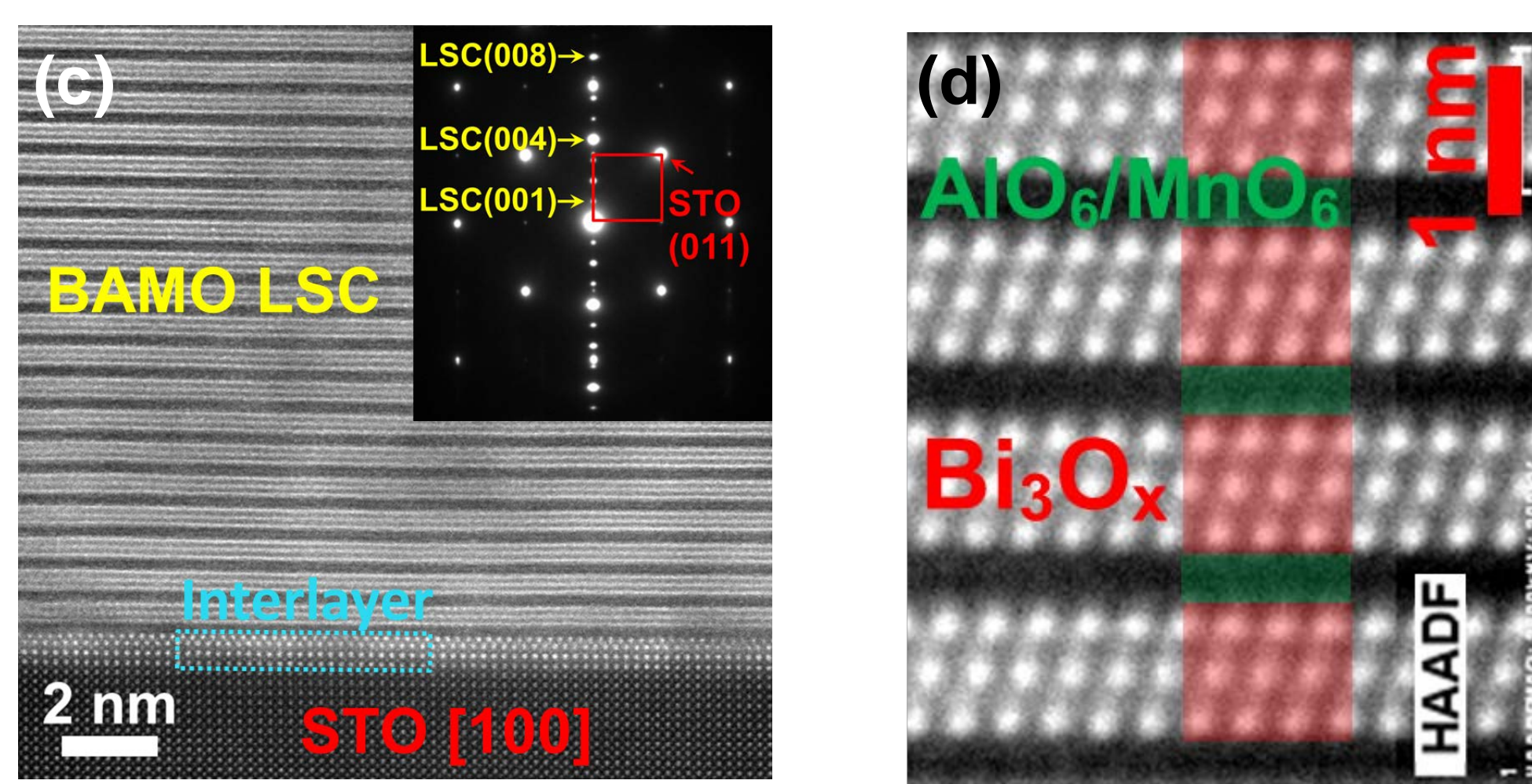


**Abstract:** Self-assembled oxide-based vertically aligned nanocomposite (VAN) thin films have aroused tremendous research interest in the past decade. The interest arises from the range of unique nanostructured films which can form and the multifunctionality arising from these forms. Hence, a large number of oxide VAN systems have been demonstrated and explored for enhancing specific physical properties, such as strain-enhanced ferroelectricity, tunable magnetotransport, and novel electrical/ionic transport properties. The epitaxial growth of the nanocomposite thin films and the coupling at the heterogeneous interfaces are critical considerations for future device applications. In another side, layered materials have sparked special research interests because of their unique anisotropic structures and rich physical phenomena as well as enormous properties in nanoscale device. Bi-Based layered supercell systems include  $\text{Bi}_2\text{AlMnO}_6$ ,  $\text{BiMnO}_3$ ,  $\text{Bi}_2\text{NiMnO}_6$ ,  $\text{Bi}_2\text{FeMnO}_6$ ,  $\text{Bi}_2\text{CoMnO}_6$ , etc, which exhibit strong ferromagnetic and piezoelectric response as well as unique optical properties at room temperature.

## Bi-Al-Mn-O Layered Supercell

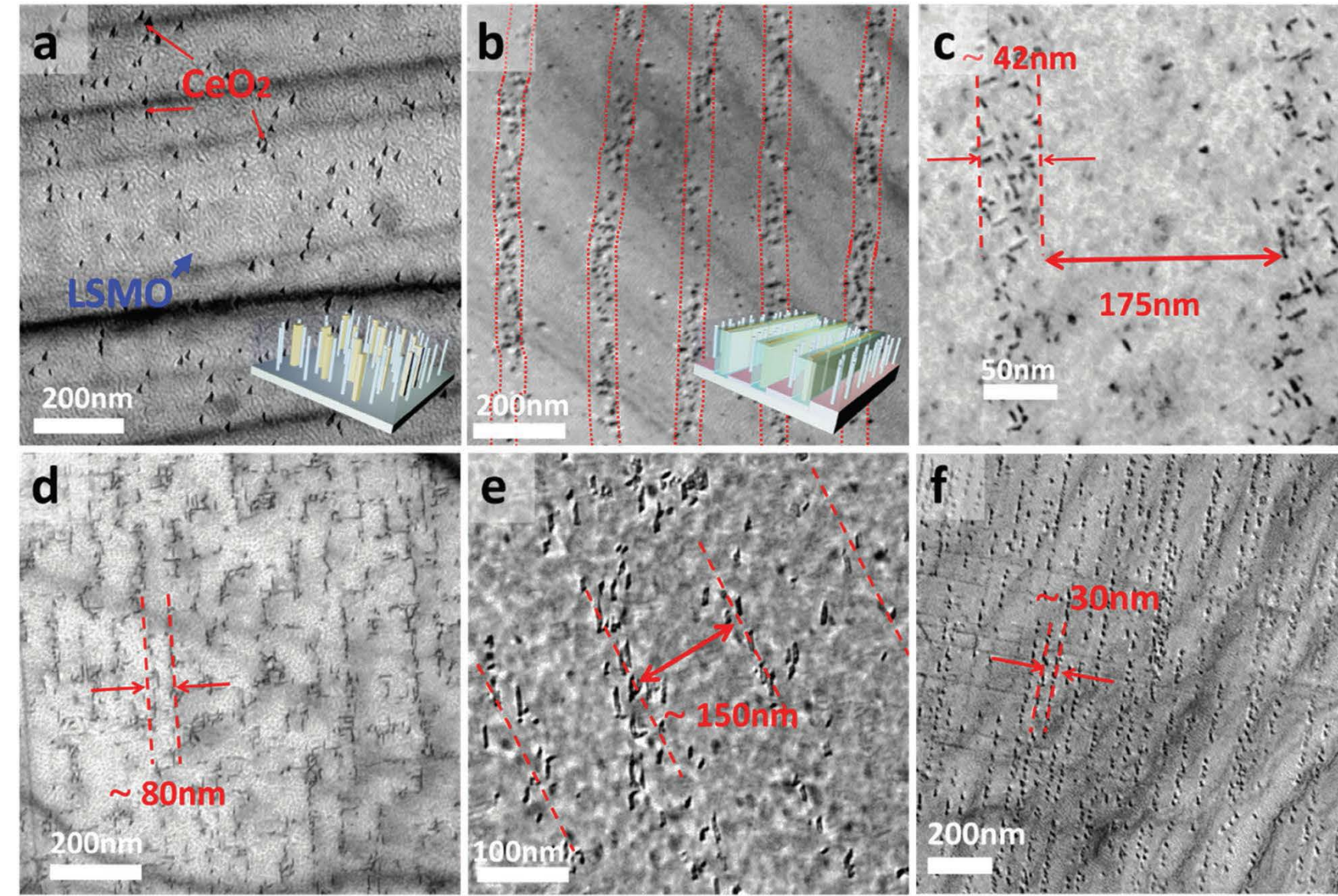


Epitaxial growth on both  $\text{SrTiO}_3$  (001) and  $\text{LaAlO}_3$  (001).

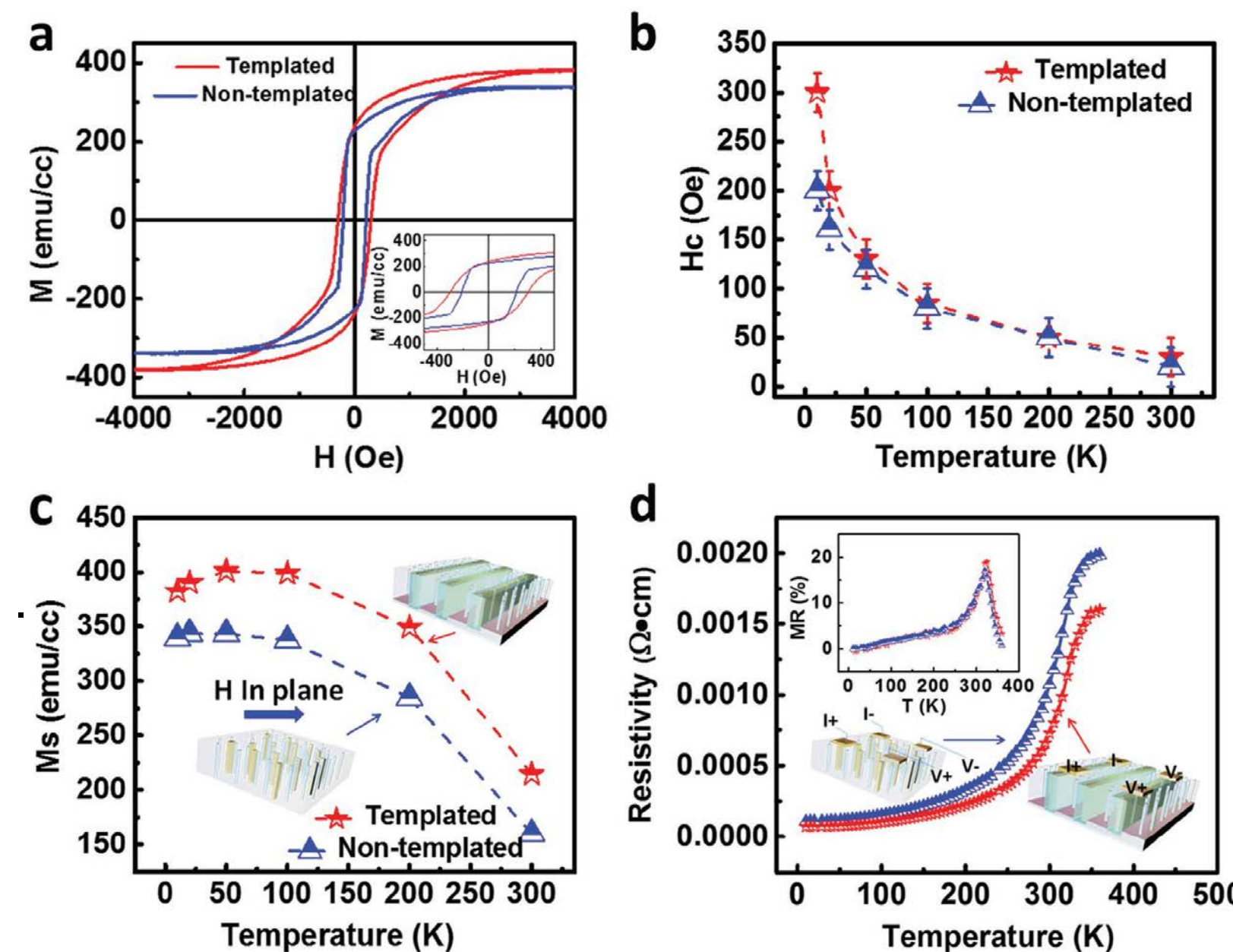


The Bi-Al-Mn-O layered supercell is composed of alternative layered stacking of  $\text{Bi}_3\text{O}_3$  and Al/Mn-O octahedral slabs along the film growth direction.

## Self-Organized Epitaxial Vertically Aligned Nanocomposites with Long-Range Ordering Enabled by Substrate Nanostructuring

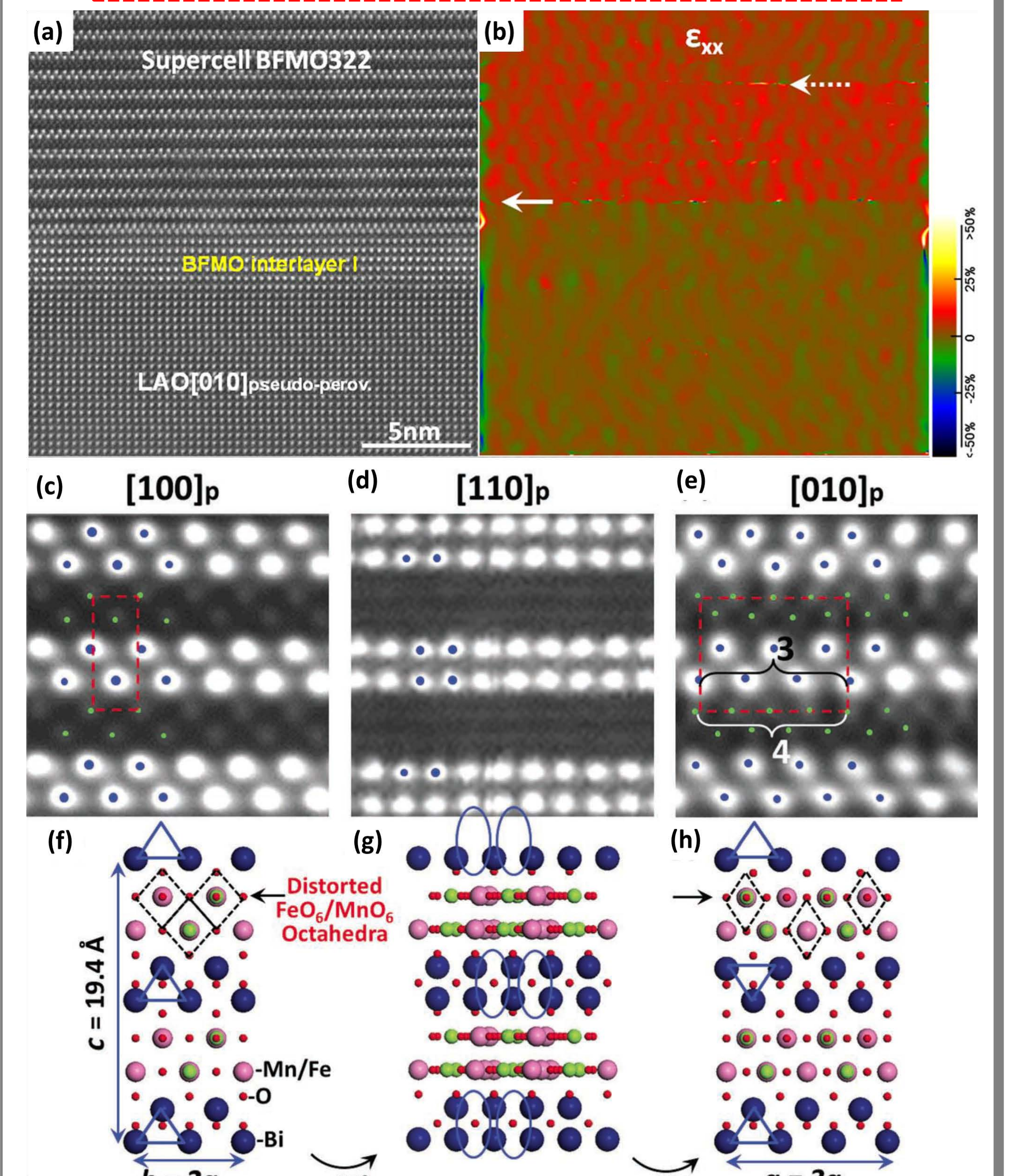


Rectangular  $\text{CeO}_2$  pillars are strongly confined and aligned in one-direction and formed ordered  $\text{CeO}_2$  rows in LSMO matrix, random while distribution of the circular  $\text{CeO}_2$  pillars/domains without any obvious long-range order has been observed on untreated STO.



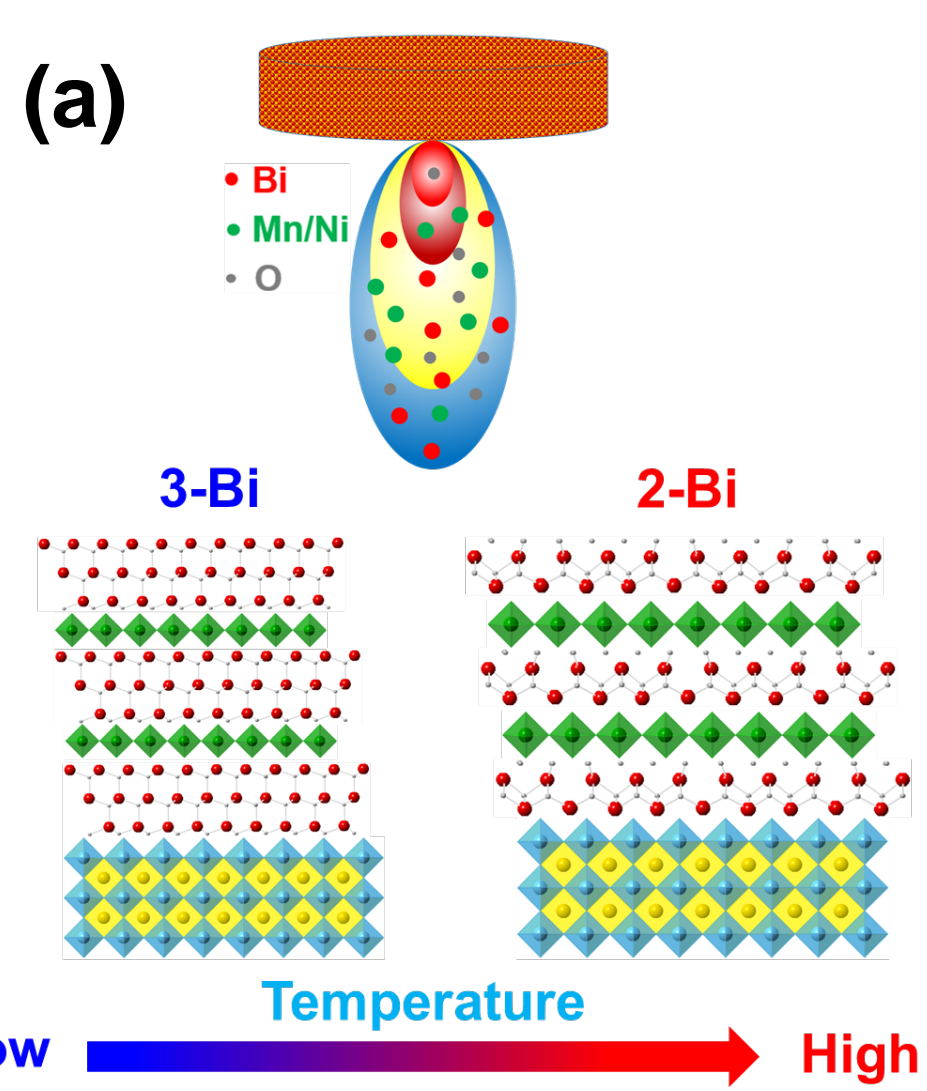
The films grown on templated substrates show obviously enhanced ferromagnetic properties; The ordered LSMO: $\text{CeO}_2$  film shows a slightly lower resistance compared to the random one, the magnetoresistance behavior is excellent for both films.

## Atomic scale TEM/STEM characterizations on thin films

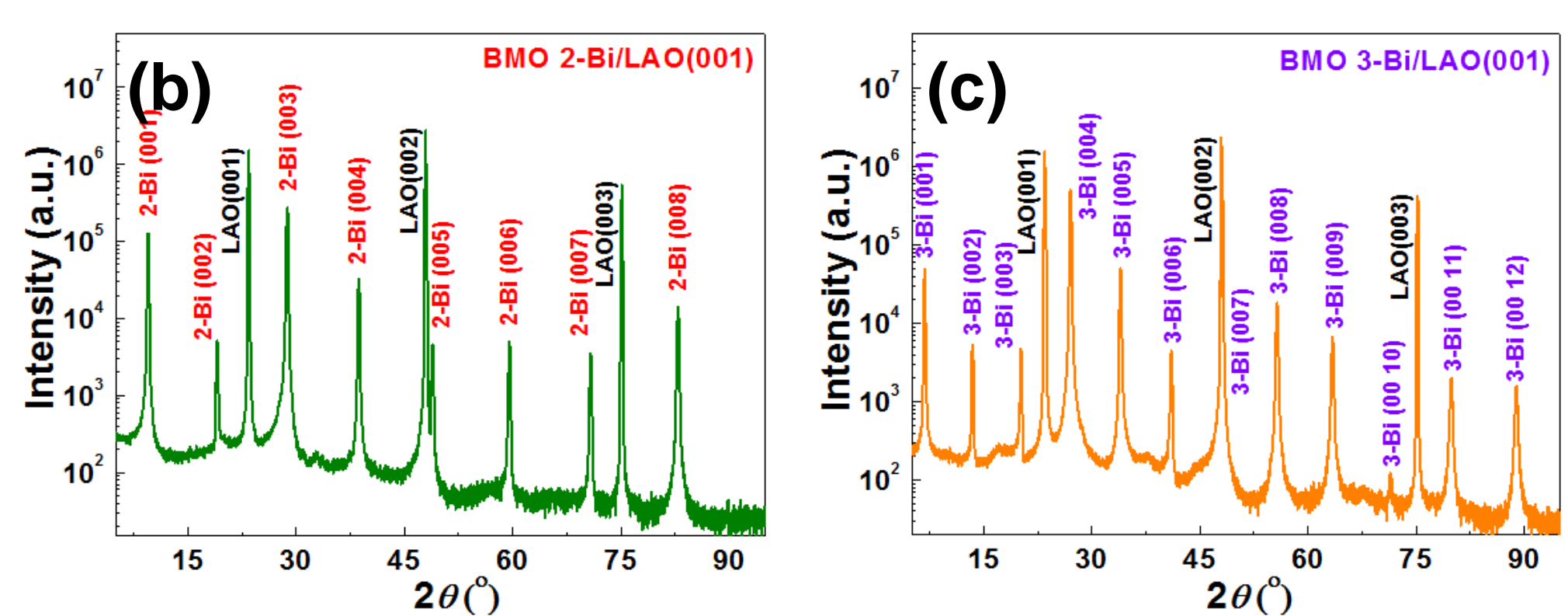


BFMO film on the pseudo-perovskite  $\text{LaAlO}_3$  (001) substrate shows a supercell (SC) structure along the  $c$ -axis. Graphic phase analysis shows a highly strained transition layers between substrate and SC. An atomic model of the novel BFMO phase with  $a = 2a_p$  ( $a_p \sim 3.99 \text{ \AA}$  stands for the lattice parameter of the pseudo-perovskite BFMO),  $b = 3a_p$  and  $c \sim 19.40 \text{ \AA}$  is proposed based on the STEM images.

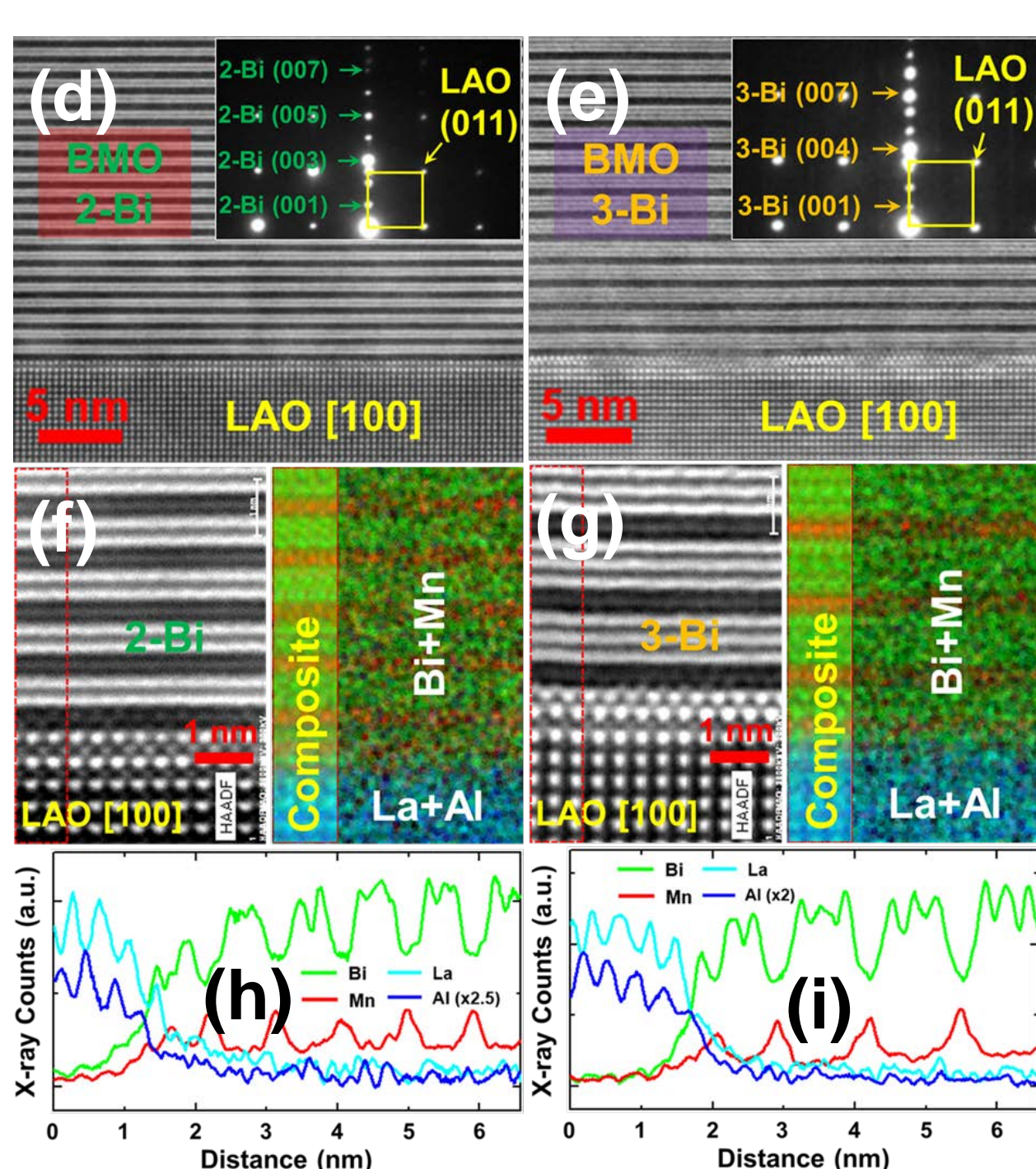
## Tunable Layered Supercell



Tunable layered structures have been achieved by precisely controlling the growth conditions.



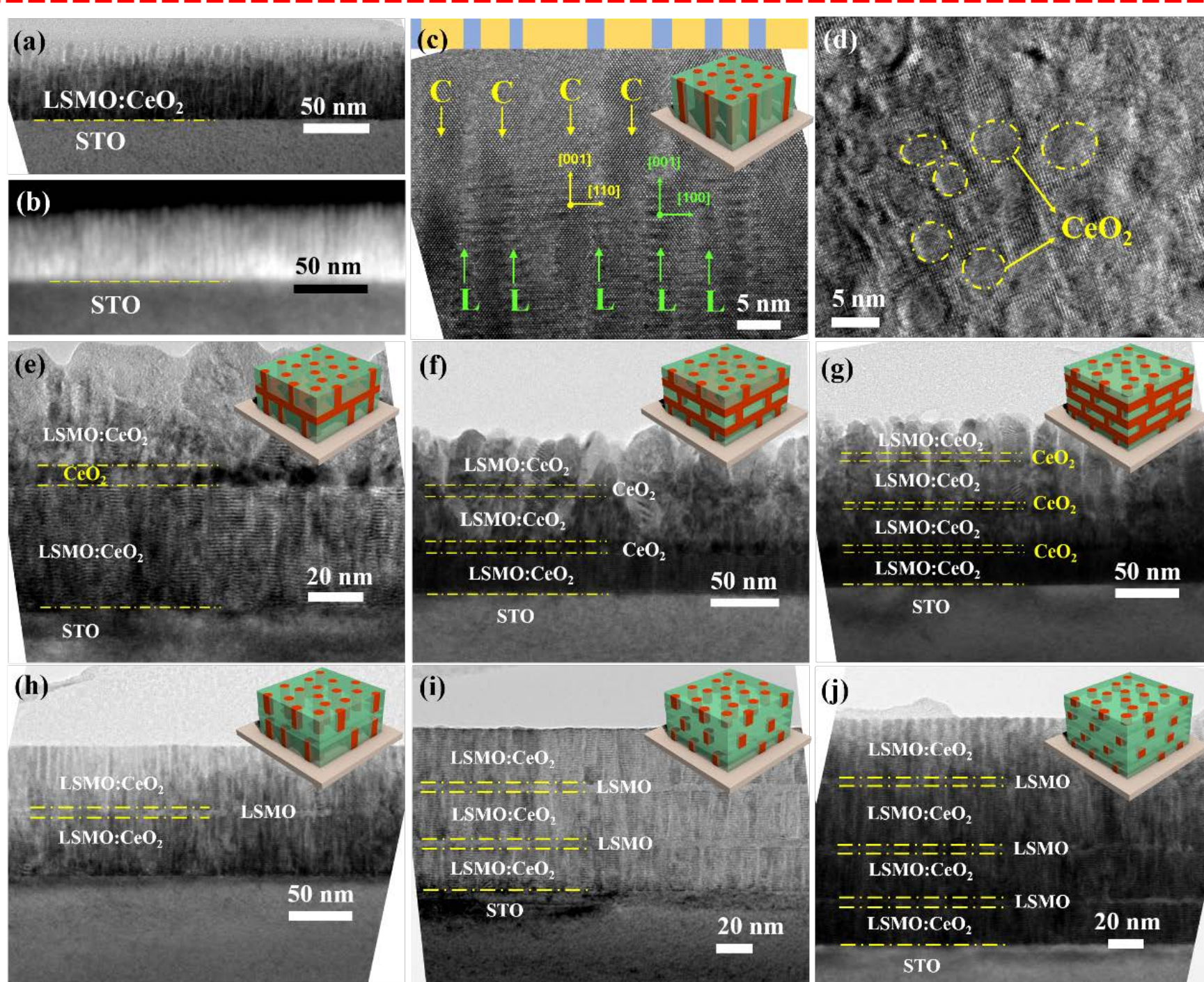
Epitaxial growth of two novel layered supercell structures from Bi-Mn-O systems.



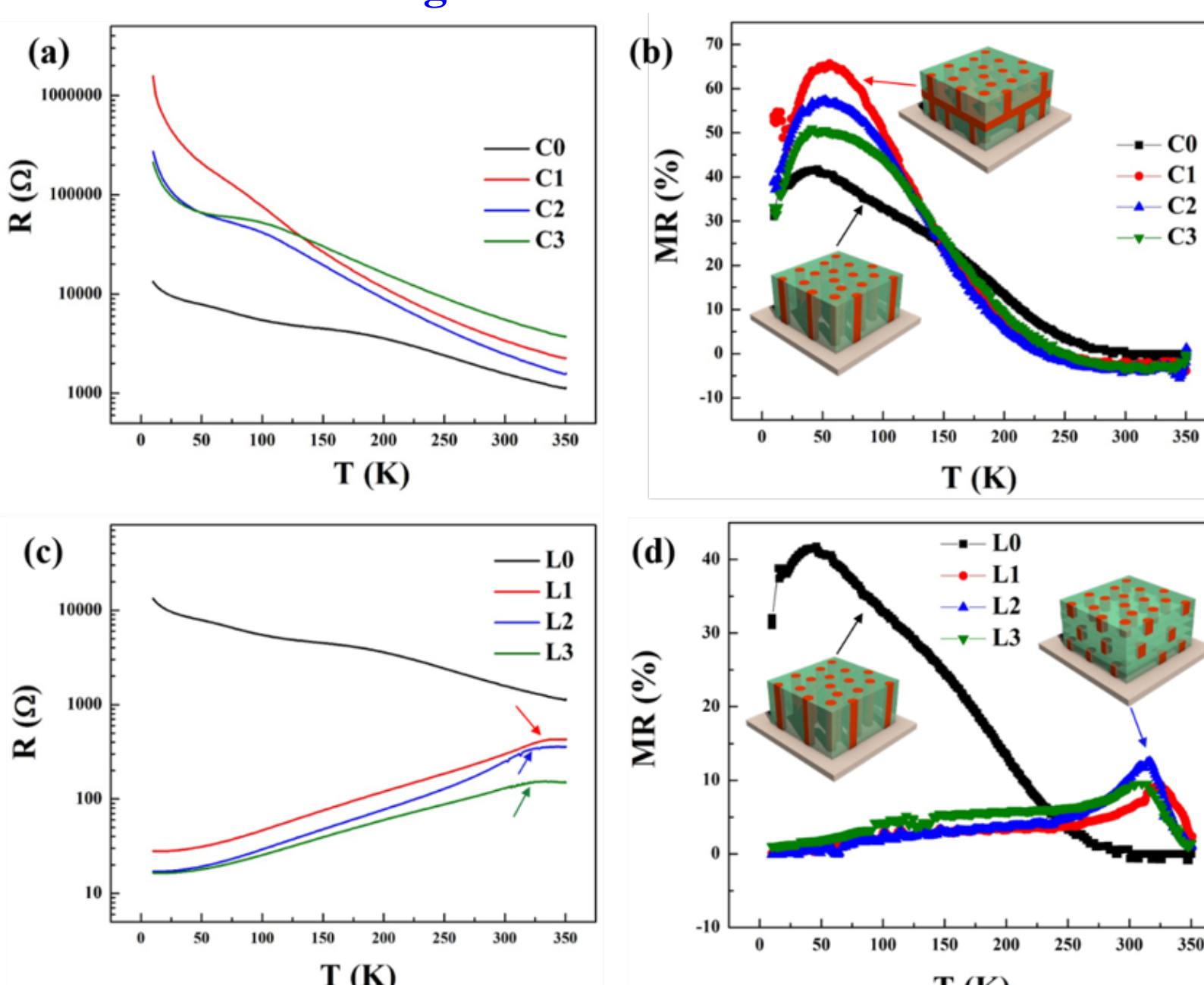
The structure of Bi-Mn-O based layered supercell can be controlled by the growth conditions.

The sublattice of Bi-Mn-O based layered structure can be tuned from two-atom-thick  $\text{Bi}_2\text{O}_3$  to three-atom-thick  $\text{Bi}_3\text{O}_3$ .

## Three-dimensional Strain Engineering in Epitaxial Vertically Aligned Nanocomposite Thin Films with Tunable Magnetotransport Properties

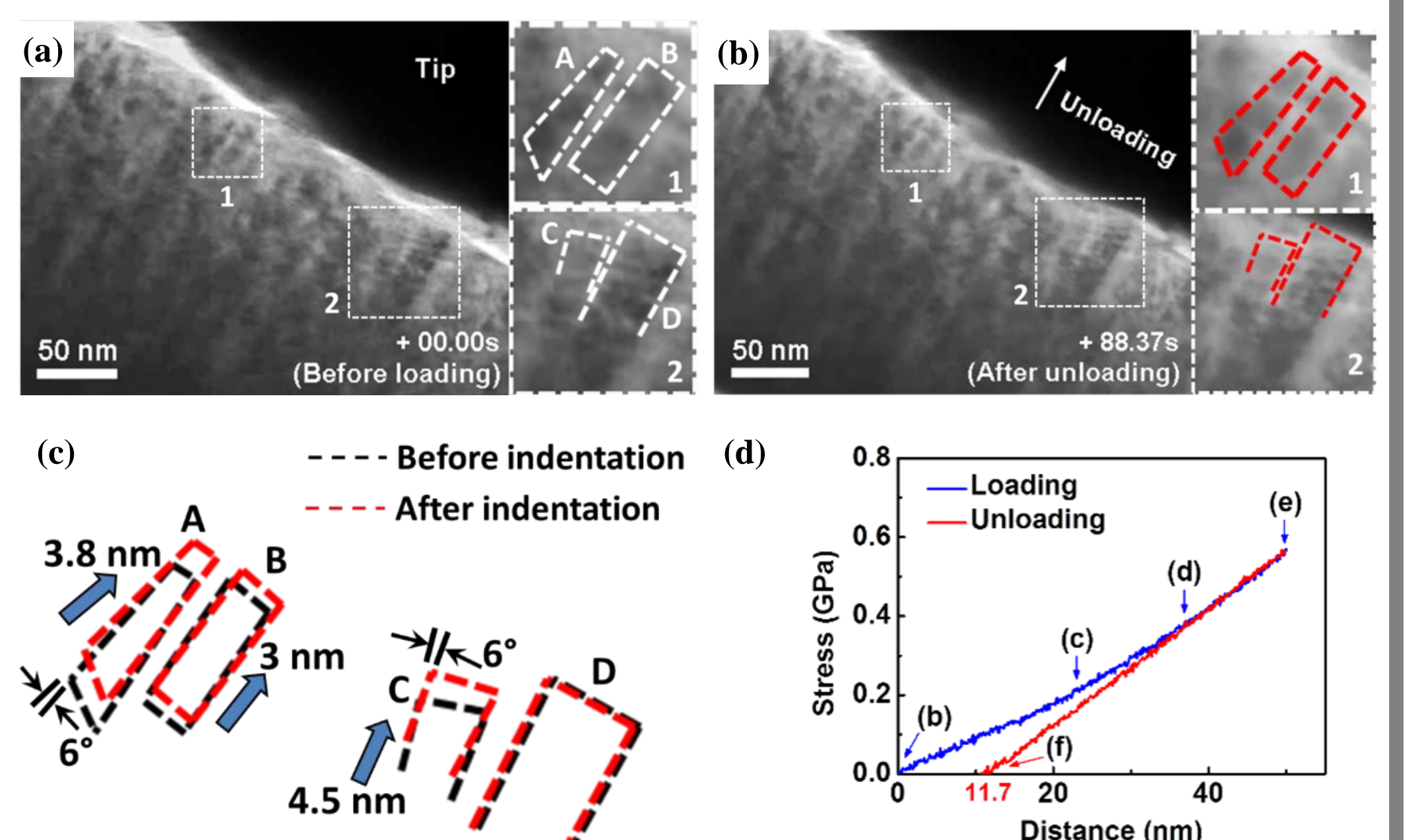


Microstructure of the designed 3-D VAN structures



Samples with  $\text{CeO}_2$  interlayer show typical semiconductor behavior, while samples with LSMO interlayer show metallic behavior, from the RT results; MR% of film C0-C3 increase firstly and then reduce as the temperature rises from low temperature to room temperature; L1-L3 structures enables higher MR values at higher temperature, e.g., 13% at 316 K in sample L2.

## In situ TEM nanoindentations on TiN thin films



In situ nanoindentations on TiN thin film with 20 nm grain size show a lot of grain activities, including grain rotation and boundary sliding, some of which are irreversible. Stress-displacement plot shows significant inelastic deformation behavior.

## References

1. A. Chen *et al.*, *Adv. Mater.*, 2013, **25**, 1028-1032
2. L. Li *et al.*, *Nano Lett.*, 2017, accepted
3. M. Fan *et al.*, *Adv. Mater.*, 2017, **29**, 1606861
4. W. Zhang *et al.*, *Nanoscale*, 2015, **7**, 13808-13815
5. A. Chen *et al.*, *Adv. Funct. Mater.*, 2011, **21**, 2423-2429
6. W. Zhang *et al.*, *ACS Appl. Mater. Interfaces*, 2015, **7**, 21646-21651
7. F. Khatkhatay *et al.*, *ACS Appl. Mater. Interfaces*, 2013, **5** (23), 12541-12547
8. J. Jian *et al.*, *Materials Science & Engineering A*, 2016, **650**, 445-453
9. W. Zhang *et al.*, *ACS Appl. Mater. Interfaces*, 2013, **5** (10), 3995-3999
10. X. Sun *et al.*, *Adv. Funct. Mater.*, submitted